ENVIRONMENTAL MONITORING WITH THE IMAGING MIMO RADARS MIRA-CLE AND MIRA-CLE X

Jens Klare, Olaf Saalmann, Helmut Wilden, Andreas R. Brenner

Fraunhofer Institute for High Frequency Physics and Radar Techniques FHR
Neuenahrer Str. 20, 53343 Wachtberg, Germany

email: jens.klare@fhr.fraunhofer.de

1. THE PRINCIPLE OF IMAGING MIMO RADAR

MIMO[1] radar is a quite new but constantly growing research field which offers some essential advantages compared to usual imaging techniques like SAR. Unlike SAR systems which need for imaging always a motion between the sensor and the scene to be observed, MIMO radars can be used also stationary to provide a continuous monitoring (24/7) of the scene of interest. Although radars with phased arrays can be used for stationary applications, they need a large number of antenna elements to achieve a reasonable image quality and resolution. These drawbacks can be smartly bypassed by using MIMO radars.

MIMO radar can be divided into two parts, namely statistical MIMO radar with widely spread transmit and receive antennas and collocated MIMO radar for imaging and GMTI[2] [1] [2] [3]. This paper addresses coherent imaging MIMO radar with collocated antennas. N_{TX} transmit antennas and M_{RX} receive antennas are arranged in a special way that all N_{TX}/M_{RX} pairs form a fully distributed virtual antenna array of $I_{virt} = N_{TX}M_{RX}$ virtual elements [4] . Each virtual antenna element is located at the center of gravity of one N_{TX}/M_{RX} pair. One essential advantage compared to phased array systems is the strongly reduced number of real antenna elements. For example, instead of using 256 antennas in a classical manner, a MIMO radar with the same array length needs only 32 antennas. Consequently, the costs could be strongly reduced and the weight reduction enables an easier transportation in difficult environmental areas. The weight reduction makes it even possible to integrate a 3D imaging MIMO radar in small UAVs[3] [5] [6] [7]. If the arrangement of the MIMO antennas is done in a suitable manner, one can even almost double the azimuth resolution compared to a phased array system of the same size.

The assignment of each TX antenna to each RX antenna can be done in different ways. One possibility is to use a time multiplexing schema by exciting one TX antenna after the other, resulting in an effective pulse repetition frequency $PRF_{eff} = PRF/N_{TX}$. Other possibilities are to use multiple orthogonal waveforms occupying the same frequency band or disjunct frequency bands [8] [9] [10]. Both increase the effective PRF and the SNR[4].

2. APPLICATIONS

Plenty of applications in the field of geoscience and remote sensing can benefit from MIMO radars. For example, stationary operated MIMO radars are able to continuously observe rock glaciers, glacier tongues, and especially the temporal variations of crevasses wich are often covered for airborne and spaceborne sensors. For wide area monitoring of glaciers, such sensors could help to fill temporal gaps which naturally exist for spaceborne monitoring programs. A constantly growing importance arises with the forecast of hillside slides, snow avalanches, debris avalanches, and rock drops due to the worldwide rising temperatures resulting in more extreme weather phenomenons and melting of the permafrost in mountainous areas. MIMO radars can provide real time 2D/3D images during day and night (24/7) at any weather in combination with change detection to image smallest changes in the range of millimeters. Also ground motions in mine areas which may result in catastrophic landslides could be monitored to support early warning systems for the citizens.

[1] Multiple-Input Multiple-Output
[2] Ground Moving Target Indication
[3] Unmanned Aerial Vehicles
[4] Signal-to-Noise Ratio

3. THE EXPERIMENTAL SYSTEMS MIRA-CLE AND MIRA-CLE X

To cover a wide range of applications, two complementary MIMO radar systems are currently developed at Fraunhofer FHR. The Ka-Band system MIRA-CLE is a fully configurable and expandable MIMO radar working at a center frequency of 36 GHz with a bandwidth of 500 MHz. Due to the chosen frequency band, MIRA-CLE is a compact and mobile system with an antenna length of just 50 cm consisting of 16 TX and 16 RX vivaldi antennas. Through adapted antenna excitation, 256 virtual antenna elements can be synthesized. Depending on the application, both the number of the antenna elements and the bandwidth can be adapted. In order to increase the SNR and the effective PRF, waveform diversity and frequency diversity techniques can be applied.

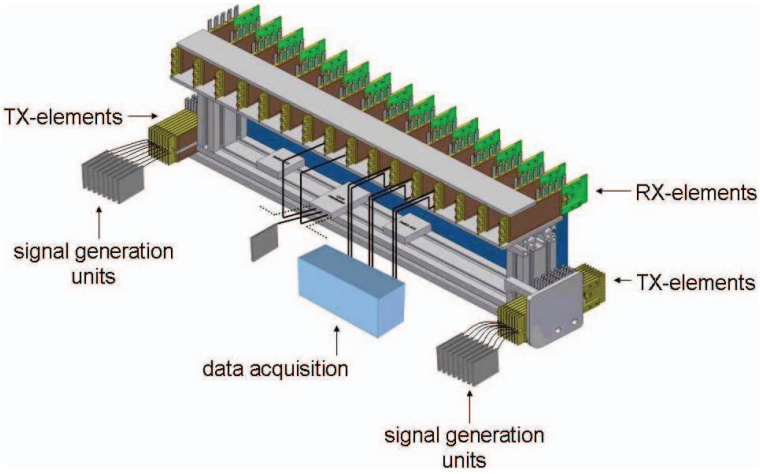

Fig. 1. Antenna configuration of the Ka-Band MIMO radar MIRA-CLE. The transmit antennas are packed at both sides of the thinned receive array.

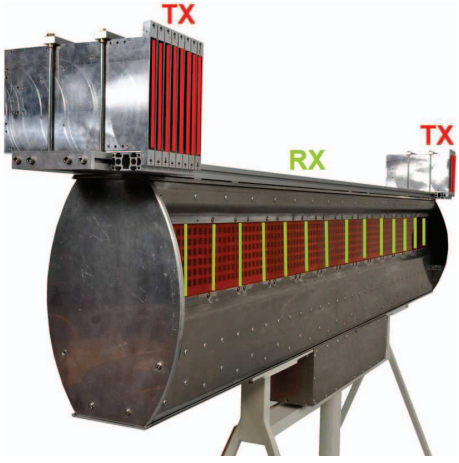

Fig. 2. Antenna configuration of the X-Band MIMO radar MIRA-CLE X

The X-Band system MIRA-CLE X works at a center frequency of 9.45 GHz with a bandwidth of 1 GHz. It uses 16 TX sector horn antennas and 14 RX patch antenna columns which result in 224 virtual antenna elements and a real antenna size of about 2 m. The radiated pulse power amounts to 33 dBm in the basic stage of extension and can be further increased by integrating more powerful amplifiers for larger range applications.

4. SIGNAL MODEL

Let's consider the geometry presented in **Figure 3**. With the distance $R = \sqrt{x_p^2 + y_p^2 + z_p^2}$ between the point scatterer P and the array center, the vector components of the unity vector $\mathbf{u}(\varphi, \theta) = (u, v, w)^T$ are given by:

$$\begin{aligned} u &= \cos\varphi\cos\theta = \frac{x_p}{R} \\ v &= \sin\varphi\cos\theta = \frac{y_p}{R} \\ w &= \sin\theta = \frac{z_p}{R} \end{aligned} \tag{1}$$

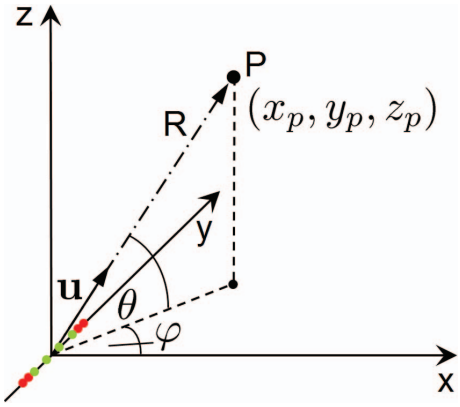

Fig. 3. Geometry of the MIRA-CLE antenna setup

Assuming far field condition, the signal which was transmitted by the radar, reflected by the point scatterer P, and finally received by the radar can be expressed after range compression by:

$$\mathbf{S}(R, \mathbf{u}) = e^{-j\frac{4\pi}{\lambda}R}\mathrm{D}^2(\mathbf{u})\mathbf{d}_{\mathrm{TX}}(\mathbf{u}) \otimes \mathbf{d}_{\mathrm{RX}}(\mathbf{u}) \tag{2}$$

with the DOA[5] vector for transmit

$$\mathbf{d}_{\mathrm{TX}}(\mathbf{u}) = \left(e^{-j\frac{2\pi}{\lambda}y_n^{\mathrm{TX}}v}\right)_{n=1\ldots N_{TX}} \tag{3}$$

and the DOA vector for receive

$$\mathbf{d}_{\mathrm{RX}}(\mathbf{u}) = \left(e^{-j\frac{2\pi}{\lambda}y_m^{\mathrm{RX}}v}\right)_{m=1\ldots M_{RX}} \tag{4}$$

$\mathrm{D}^2(\mathbf{u})$ denotes the two-way antenna characteristics of a single TX/RX element and $\otimes$ is the Kronecker product. One can resolve the data in angle by using digital beamforming with the vector $\mathbf{g}^*$ focused to the direction defined by v_0:

$$\begin{aligned} s(R, v_0) &= \mathbf{g}^*(v_0) \cdot \mathbf{S}(R, \mathbf{u}) \\ &= \sum_{i=1}^{I_{virt}} e^{j\frac{4\pi}{\lambda}y_i^{virt}v_0} \cdot S_i(R, \mathbf{u}) \\ &= e^{-j\frac{4\pi}{\lambda}R} \cdot \mathrm{D}^2(\mathbf{u}) \cdot \sum_{i=1}^{I_{virt}} e^{j\frac{4\pi}{\lambda}y_i^{virt}(v_0 - v)} \end{aligned} \tag{5}$$

5. EXPERIMENTAL RESULTS

This section will be filled in the final paper. We will present and analyze results of different experiments performed at hilly locations (e. g. vineyards). The potential of the presented systems regarding to change detection will be investigated too.

[5]Direction Of Arrival

6. REFERENCES

[1] J. Li, P. Stoica, and X. Zheng, "Signal synthesis and receiver design for MIMO radar imaging," *Signal Processing, IEEE Transactions on*, vol. 56, no. 8, pp. 3959–3968, Aug. 2008.

[2] D. W. Bliss, K. W. Forsythe, S. K. Davis, G. S. Fawcett, D. J. Rabideau, L. L. Horowitz, and S. Kraut, "GMTI MIMO radar," in *Proc. International Waveform Diversity and Design Conference*, 2009, pp. 118–122.

[3] A.M. Haimovich, R.S. Blum, and L.J. Cimini, "MIMO radar with widely separated antennas," *Signal Processing Magazine, IEEE*, vol. 25, no. 1, pp. 116–129, 2008.

[4] J. H. G. Ender and J. Klare, "System architectures and algorithms for radar imaging by MIMO-SAR," in *IEEE RadarCon 2009*, Pasadena, USA, May 2009.

[5] J. Klare, M. Weiss, O. Peters, A. R. Brenner, and J. H. G. Ender, "ARTINO: A new high resolution 3D imaging radar system on an autonomous airborne platform," in *Proc. IEEE International Conference on Geoscience and Remote Sensing Symposium IGARSS 2006*, Denver, USA, July 2006, pp. 3842–3845.

[6] J. Klare, A. R. Brenner, and J. H. G. Ender, "A new airborne radar for 3D imaging - image formation using the ARTINO principle," in *Proc. EUSAR 2006*, Dresden, Germany, May 2006, p. ID 103.

[7] J. Klare, D. Cerutti-Maori, A. R. Brenner, and J. H. G. Ender, "Image quality analysis of the vibrating sparse MIMO antenna array of the airborne 3D imaging radar ARTINO," in *Proc. IEEE International Geoscience and Remote Sensing Symposium IGARSS 2007*, Denver, USA, July 2007, pp. 5310–5314.

[8] D.W. Bliss, K.W. Forsythe, and C.D. Richmond, "MIMO radar: Joint array and waveform optimization," *Signals, Systems and Computers, 2007. ACSSC 2007. Conference Record of the Forty-First Asilomar Conference on*, pp. 207–211, Nov. 2007.

[9] D. J. Rabideau, "Adaptive MIMO radar waveforms," *Radar Conf. 2008. Proc. of the IEEE, pp. 1349-1354, May 2008.*, pp. 1349–1354, May 2008.

[10] J. Klare, "Digital beamforming for a 3D MIMO SAR - improvements through frequency and waveform diversity," in *Proc. IEEE International Geoscience and Remote Sensing Symposium IGARSS 2008*, Boston, USA, July 2008, pp. V 17–20.